*Manuscript
Click here to view linked References

HYALURONAN MEDIATES THE ADHESION OF PORCINE PERIPHERAL BLOOD MONONUCLEAR CELLS TO POLY (I:C)-TREATED INTESTINAL CELLS AND MODULATES THEIR CYTOKINE PRODUCTION

María José Docampo[1], Jennifer Cabrera, and Anna Bassols*

Departament de Bioquímica i Biologia Molecular, Facultat de Veterinària, Universitat Autònoma de Barcelona, 08193 Bellaterra, Barcelona, Spain.

* Corresponding author: Tel.: +34 93 581 1042; fax: +34 93 581 2006.

E-mail address: anna.bassols@uab.cat

[1] Present address: Neuroimmunology and Multiple Sclerosis Research, Klinik für Neurologie, Universitätsspital Zürich, CH-8091 Zürich, Switzerland

ABSTRACT

Hyaluronan (HA), a major component of the extracellular matrix (ECM), has been increasingly recognized as a regulator of inflammation. Its role is complex since it has pro- and anti-inflammatory actions by modulating the expression of inflammatory genes, the recruitment of inflammatory cells and the production of inflammatory cytokines, but also by attenuating the course of inflammation and providing protection against tissue damage. Certain viruses and other inflammatory stimuli induce organization of HA into cable-like structures, which may be responsible for leukocyte recruitment and, on the other hand, low molecular weight fragments of HA have been shown to activate various inflammatory responses.

The aim of the present study was to analyze the effects of a simulated infection with the viral mimetic Poly (I:C) on HA deposition on different porcine intestinal cells (primary colonic muscular smooth muscle cells (SMC), and epithelial IPEC-J2 and IPI-2I cell lines) and on the recruitment of peripheral blood mononuclear cells (PBMC) to intestinal cell layers. We show that Poly (I:C) treatment induces the formation of an HA-based pericellular matrix coat in muscular SMC and in intestinal epithelial cells (IECs) and that, on differentiated IPEC-J2 cells, HA accumulates in the basolateral membrane. Porcine PBMCs bind to Poly (I:C)-treated cells and this binding is dependent on HA, since the increase in adhesion is abolished by hyaluronidase treatment of the cell layers. A second goal was to study the effect of different molecular weight HA forms on the production of pro-inflammatory cytokines and chemokines (TNF-α, IL-1β~~, IL-6~~ and IL-8) by porcine PBMCs. Low molecular weight HA fragments (100-150 kDa), in contrast to high molecular weight HA (2500 kDa), stimulate the release of these pro-inflammatory mediators by porcine PBMCs. Our results suggest that HA is involved in the inflammatory response against pathogenic insults to the porcine gut.

Key words: Hyaluronan; Poly (I:C); intestinal cells; PBMCs; cytokines; inflammation; pig

1. INTRODUCTION

Hyaluronan or hyaluronic acid (HA) is a glycosaminoglycan polymer composed of repeating disaccharide units of D-glucuronic acid and N-acetyl-D-glucosamine, and it is a major constituent of the extracellular matrix (ECM). HA, which is secreted by many cell types, is assembled at the plasma membrane by HA synthases (HAS) and extruded into the extracellular space. HA degradation typically occurs at the cellular level by a mechanism involving the cell surface receptor CD44 and hyaluronidases (HYAL). However, HA may also be degraded at sites of inflammation by reactive oxygen species and secreted hyaluronidases of bacterial origin (Stern et al., 2007). Beyond its physical properties as a structural ECM molecule, HA provides cellular cues to regulate inflammation and tissue repair (Petrey and de la Motte, 2014). The biological activity of HA is dependent upon its molecular mass. Large HA polymers support tissue structure and integrity due to their hygroscopic and viscoelastic properties and serve to suppress the inflammatory response. In response to injury and inflammation, HA undergoes increased synthesis through induction of HAS and degradation to smaller molecular mass fragments by hyaluronidases (Jiang et al., 2011). Overall, HA in its fragmented form is a reflection of tissue under stress and exert pro-angiogenic, inflammatory, and immunostimulatory effects mediated by binding to its receptors (Erickson and Stern, 2012). CD44 is the main cell surface HA receptor (Aruffo et al., 1990) and is expressed on the plasma membrane of most cells. In addition to binding to CD44 and other receptors, HA also binds to Toll-like receptor (TLR) 2 and 4 (TLR2 and TLR4), components of the innate immune system (Jiang et al., 2007). Thus, HA exists as both a pro- and anti-inflammatory molecule *in vivo*, these contradictory functions being determined by polymer length and the receptors HA engages.

Increased accumulation of HA, together with leukocyte recruitment is a consistent feature during inflammatory diseases (Petrey and de la Motte, 2014), including

intestinal- affecting processes such as inflammatory bowel disease in humans (de la Motte et al., 2003) or experimental dextran sulfate sodium-induced colitis in rats (Kessler et al., 2008). Infection with respiratory syncytial virus (RSV) or measles virus also increase cell surface HA (De La Motte et al., 1999). In several cell types *in vitro*, cellular stress induced by virus or the double stranded RNA viral mimic polyinosinic:polycytidylic acid (Poly (I:C)), other ER stressors or hyperglycemia increase cell surface HA deposition and the formation of long cable-like structures that are important for leukocyte attachment since they have binding properties not featured by the normal HA found in the pericellular glycocalyx (De La Motte et al., 1999; Evanko et al., 2009; Jokela et al., 2008; Lauer et al., 2009; Majors et al., 2003; Stober et al., 2014; Potter-Perigo et al., 2010; Wang and Hascall, 2004). Adhesion of leukocytes to these HA forms is mediated by binding to the receptor CD44 (De La Motte et al., 1999). It is believed that these cable-like structures correspond *in vivo* to cross-linked forms of HA that would constitute a protective mechanism for tissues undergoing inflammation by keeping immune cells bound to these matrices in an inactivated state (Day and de la Motte, 2005).

On the other side, HA has been shown to undergo rapid degradation at sites of inflammation and low molecular weight degradation products are able to elicit various proinflammatory responses in immune cells and other cell types, at least in part through TLR4 (Termeer et al., 2002; Taylor et al., 2004; Yamawaki et al., 2009; Campo et al., 2010; Jiang et al., 2011).

Infectious diseases are of great importance for pig industry due to increased medication costs and decreased food conversion or even death of the animals, all leading to high economic losses. The involvement of HA and other ECM components in the modulation of inflammation has become increasingly evident over the years, however, little is known about the role of HA as mediator of inflammation in porcine cells.

The objectives of the present study have been a) to investigate the effect of the viral mimetic Poly (I:C) on HA deposition on different porcine intestinal cells (primary colonic muscular smooth muscle cells (SMCs), and intestinal epithelial IPEC-J2 and IPI-2I cells lines, and b) to study the effects of different molecular weight HA forms on the production of pro-inflammatory mediators (TNF-α, IL1-β, IL-6 and IL-8) by porcine PBMCs.

2. MATERIALS AND METHODS

2.1. Cell lines and cell culture

Porcine intestinal epithelial cell (IEC) lines IPI-2I and IPEC-J2 were obtained from Dr. Cristina Arce (Universidad de Córdoba, Spain) and Prof. Anthony Blikslager (North Carolina State University, Raleigh, NC, USA). The IPEC-J2 is a non-transformed cell line derived from the epithelium of a neonatal, unsuckled piglet jejunum (Rhoads et al., 1994). The IPI-2I is an SV40-immortalized cell line derived from the ileum of an adult boar (Kaeffer et al., 1993). IPEC-J2 cells were cultured in Dulbecco's Modified Eagle Medium (DMEM)/Ham's F-12 (1:1) medium (Invitrogen TM Life Technologies, Carlsbad, CA, USA) supplemented with 5% fetal calf serum (FCS), 100 U/ml penicillin and 100 µg/ml streptomycin (all from PAA Laboratories GMbH, Pasching, Austria). IPI-2I cells were cultured in DMEM/F-12 (1:1) medium supplemented with 10% FCS, 4mM L-glutamine (PAA), 100 U/ml penicillin and 100 µg/ml streptomycin. Cells were grown in a humidified atmosphere at 37ºC with 5% CO_2. IPEC-J2 cells were used between passages 65-85; IPI-2I cells were used between passages 40-65.

Porcine primary colon mucosal smooth muscle cells (SMCs) were prepared as described by de la Motte *et al*. (2003) with modifications. Colon samples were obtained from 6-month old Large White healthy pigs undergoing experimental surgery at the Facultat de Veterinària (UAB). Samples were thoroughly rinsed with sterile PBS in

132 order to remove any remaining blood and lumen content. After cleaning, the muscle
133 cell layer was removed, minced and digested in medium with 0.2 mg/ml type IA
134 collagenase from *Clostridium histolyticum* (Sigma, St. Louis, MO), 0.1 mg/ml DNase
135 (Roche, Manheim, Germany), 250 U/ml penicilin, 250 µg/ml streptomycin (PAA) and
136 0.625 µg/ml fungizone for 3 h at 37ºC under agitation. The supernatant was separated
137 from the rest of non-digested tissue and centrifuged at 300 g for 10 minutes. The
138 resulting pellet was resuspended in DMEM/F-12 culture medium supplemented with
139 10% FCS, 250 U/ml penicilin, 250 µg/ml streptomycin and 0.625 µg/ml fungizone and
140 seeded in 25 cm^2 culture flasks and cultured in a humidified atmosphere at 37ºC with
141 5% CO_2. All the procedure was performed under sterile conditions. The identity of SMC
142 was confirmed by immunocytochemistry using an antibody against α-SMA. Primary
143 cells were used between passages 2 and 4.
144
145 **2.2. Treatment of cells with Poly (I:C) and HA staining**
146 Porcine primary colon mucosal SMCs and IEC lines (IPI-2I and IPEC-J2) were seeded
147 in 24-well plates containing coverslips in the corresponding culture medium (2 x 10^4
148 cells/well and 5 x 10^4 cells/well respectively) and left overnight for attachment. Then
149 the culture medium was removed and replaced by fresh culture medium containing 20
150 µg/ml of Poly (I:C) for 18 h. Control cells were incubated in parallel in culture medium
151 without the viral mimic.
152 After treatment, cells were rinsed with phosphate-buffered saline (PBS) and fixed in
153 methanol for 5 minutes at -20ºC. After rinsing with PBS, non-specific binding sites were
154 blocked with 1% BSA in PBS for 30 minutes at room temperature. Cells were then
155 incubated with 1 µg/ml of biotinylated hyaluronan-binding protein (HABPb) (Seikagaku,
156 Tokyo, Japan) in PBS containing 0.1% BSA overnight at 4ºC. Subsequently, cells were
157 washed in PBS and incubated with streptavidin Alexa-488 (Molecular Probes,
158 Invitrogen, Eugene, OR) 1 in 1000 dilution in PBS. Nuclei were visualized by incubating

samples with 10 μg/ml bisbenzimide trihydrochloride (Hoechst 33342, Sigma) for 3 minutes. Cells were washed and mounted in Fluorsave mounting medium (Calbiochem). Slides were examined using a confocal laser scanning microscope Olympus FluoView^{TM} FW1000 (Olympus, Hamburg, Germany) with an objective Plan Apo 60x (NA 1.4, oil) using the Olympus FW10-ASW version 1.7.c software (Olympus). Alternatively, after incubation with the HABPb, cells were incubated with avidin-biotin-peroxidase complex (Immunopure ABC Standard Peroxidase Staining Kit, Pierce, Rockford, Illinois, USA. The reaction was developed using 3,3'-diaminobenzimide as peroxidase substrate (Liquid DAB+Substrate Chromogen System, Dako) and cells were counterstained with Mayer's haematoxylin (Merck, Darmstad, Germany). Cells were washed in tap water for 10 minutes, dehydrated in increasing concentrations of alcohols and mounted in DPX mounting medium (Sigma). Cells were examined with a Leica DM-6000 microscope and photographed with an integrated Leica DFC480 digital camera system using the Leica IM50, Version 4.0 Release 117 software (Leica Microsystems, Wetzlar, Germany).

Controls for specificity of HA staining included digestion of the cells with 2 U/ml of hyaluronidase from *Streptomyces hyalurolyticus* (Sigma) in 50 mM NaOAc 150 mM NaCl pH 6 buffer for 1 hour at 37ºC prior incubation with the HABPb.

2.3. Polarisation of IPEC-J2 cells

IPEC-J2 cells were seeded on 12 mm diameter Transwell collagen-coated PTFE filters of pore size 0.4 μm (Corning, The Netherlands) at a high density (5 x 10^5 cells/insert) to saturate the membrane and reduce the need for cell division (Geens and Niewold, 2011; Vergauwen, 2015). Every other day, culture medium was refreshed. The formation of a polarised monolayer was monitored by measuring the transepithelial electrical resistance (TEER), which monitors confluence and presence of tight junctions. TEER measurements were performed using a Millicell ERS-2 electrical resistance system with STX1 electrodes (Millipore, Germany) (Servei de Cultius

Cel·lulars, Producció d'Anticossos i Citometria, UAB) and expressed as Ω x cm2. Blank Transwell inserts were run in conjunction with cultures to correct for background.

After 13 days in culture, when TEER values maintained stable over time, cells were treated with 20 μg/ml of Poly (I:C) for 18h as described above. Control cultures were incubated in parallel in culture medium without the viral mimic. TEER values were recorded after Poly (I:C) treatment and cells were then fixed 4% paraformaldehyde for 20 min at 37ºC, rinsed in PBS, permeabilized with 0.1 % Triton X-100 in PBS for 10 min and stained for HA as described above. Membranes were detached from the insert, mounted on glass slides with Fluorsave and analyzed with a Leica TCS SP5 AOBS laser scanning confocal microscope (Servei de Microscòpia, UAB) and the IMARIS software.

2.4. Isolation of porcine peripheral blood mononuclear cells (PBMCs)

Blood samples from 6 month old Large White healthy pigs were collected in heparinized tubes and PBMCs were separated by density gradient centrifugation using Vacutainer CPT™ tubes (BD Biosciences). Washed cells were resuspended in RPMI-1640 medium (Sigma) supplemented with 10% FCS, 1% non-essential aminoacids, 1 mM sodium pyruvate (Sigma), 100 U/ml penicillin and 100 μg/ml streptomycin (PAA, GE Healthcare).

2.5. Assay for PBMC adhesion to porcine IECs

Porcine IECs (IPI-2I and IPEC-J2) were seeded in 96-well plates at $5x10^4$ cells/well density in the corresponding culture medium. After 24 h, the medium was removed and replaced by fresh culture medium with either no addition or 20 μg/ml of Poly (I:C) for 18h.

Prior to the assay, porcine PBMCs (10×10^6/ml) were incubated with 5 μg/ml calcein-AM (Molecular Probes, Invitrogen) for 30-45 min at 37ºC and then washed twice in

RPMI medium without phenol red (Sigma) and resuspended to 3 × 10^6/ml. Some wells were treated with 0.66 U/ml of hyaluronidase from *Streptomyces hyalurolyticus* (Sigma) for 20-30 min prior to the adhesion assay. Then, 100 μl of PBMC suspension was added to the porcine IEC cell monolayers and allowed to adhere for 90 min at 4ºC. Plates were washed gently three times with cold medium, and visualized to ensure monolayer integrity, before measuring the plate in a Viktor 3 FusionTM Series Universal Microplate Analyser (Perkin Elmer, Waltham, MA, USA) with excitation and detection wavelengths of 485 and 535 nm, respectively. Six replicates of each condition were used. Results were plotted against a standard curve made with serial dilutions of calcein-stained PBMCs, with 4 replicates of each. Statistical significance was determined using the Student's *t* test. Values of $p \leq 0.05$ were considered to be significant.

For imaging experiments, the same assay was conducted in cells seeded on coverslips in 24-well plates. After adhesion, cells were fixed in methanol at -20ºC for 5 minutes, rinsed in PBS and blocked with 1% BSA and 20% normal goat serum (NGS) in PBS for 1 h at RT. Cultures were then simultaneously incubated with 1 μg/ml HABPb and either mouse monoclonal anti-porcine CD44 antibody (VRM, Pullman) (1 in 100), monoclonal mouse IgG1 anti-swine CD172a (hybridoma undiluted), rabbit polyclonal anti-human CD20 antibody (Cultek) (1 in 100), or rabbit polyclonal anti-human CD3 (Dako) in 0.1% BSA in PBS. Cells were then rinsed in PBS and incubated with a mixture of streptavidin Alexa Fluor®488 1 in 100 dilution and Alexa Fluor®568 goat anti-mouse or anti-rabbit IgG 1 in 500 dilution and in PBS for 1 h at RT. Nuclei staining and mounting was performed as described above. PBMCs smeared in silane-coated slides and fixed with methanol were used as positive controls for these cell markers. Samples were visualized and analysed with a Leica TCS SP5 AOBS laser scanning confocal microscope and processed using the IMARIS software.

2.6. ELISA assay for cytokine quantification

Porcine PBMCs were plated in 96-well plates ($5x10^5$ cells/well) and incubated with either low-molecular weight HA (LMW-HA, 100-150 kDa) from pig skin (Sigma) or high molecular weight HA (HMW-HA, Select-HA 2500K, Sigma) at 0.1 and 0.4 mg/ml or with 1 μg/ml of LPS (lypopolysaccharides from *Escherichia coli* 055:B5, Sigma) for 24 h at 37°C and the supernatant was harvested, centrifuged at 3000 g for 10 min to clarify debris and cells, and stored at -20°C until needed. The concentrations of TNF-α, IL1β, IL-6 and IL-8 were measured in PBMC culture supernatants using commercially available sandwich enzyme-linked immunosorbent assay (ELISA) kits using tetramethylbenzidine as peroxidase substrate (Quantikine, R&D systems, Minneapolis, MN), according to the manufacturer's recommended protocols. The absorbance values were detected at 450 nm wave-length using a iEMS Reader MF photometric microplate reader and the concentrations were determined according to the standard using Ascent software (version 2.6) for iEMS Reader MF (Thermolabsystems). For each condition we used 6 wells and supernatant from duplicated wells were pooled and measured together, resulting in triplicates for each condition. Each sample was measured by duplicate and the average concentration was considered. Statistical significance was determined using the Student's *t* test. Values of $p \leq 0.05$ were considered to be significant.

3. RESULTS

3.1. Effects of Poly (I:C) treatment on HA deposition in porcine intestinal cells

Both IEC lines, IPI-2I and IPEC-J2, produce very little amount of HA in basal conditions as assessed by cytochemistry, whereas in the primary culture of mucosal SMCs a larger production of the polysaccharide is observed. After Poly (I:C) treatment, an increase in HA is noticed, especially in IPI-2I and primary SMCs. Cell localization appears to be different since in IPI-2I cells HA shows a pericellular staining whereas in

primary SMCs, HA is located near the cell membrane and expands forming cable-like structures between cells in close vicinity (Figure 1A). To better appreciate these differences, HA was labeled by fluorescent staining and visualized by confocal microscopy. With this staining procedure, an increase in HA production and changes in its structure were clearly observed (Figure 1B).

To assess the cellular distribution of HA in polarised intestinal cells, the effects of Poly (I:C) on IPEC-J2 grown on collagen-coated Transwell membranes were studied. In these conditions, IPEC-J2 cells undergo differentiation into a polarised monolayer phenotype, which is a good model to investigate intestinal epithelial function due to its similarities with IECs *in vivo* (Geens and Niewold, 2011; Vergauwen, 2015). The formation of a polarised monolayer was monitored by measuring the transepithelial electrical resistance (TEER). After 13 days of culture, TEER values remained stable over time indicating a fully differentiated monolayer (Geens and Niewold, 2011; Schierack et al., 2006). At this time point, with TEER values of 3559 ± 293 Ω x cm2 (mean ± SEM; n=18) cells were challenged with Poly (I:C).The viral mimic caused a significant drop in TEER values (771 ± 54 Ω x cm2) compared to untreated cells (3519 ± 454 Ω x cm2) (Fig 2A), indicating that the treatment disrupts the epithelial monolayer integrity. As clearly shown in confocal images, these changes were accompanied by a dramatic increase in basolateral HA production by these cells (Fig 2B). Noteworthy, HA induction in this culture system is much more evident than that observed in non-polarised IPEC-J2 cells.

3.2. Adhesion of PBMCs to porcine intestinal epithelial cells mediated by HA

IECs were treated with Poly (I:C) and the effect on PBMC adhesion to the cell layer was quantitatively assessed by a fluorometric assay after loading the PBMC with the fluorescent stain calcein and letting these cells to adhere to the epithelial cells (Figure 3). With this assay, it is clearly observed that Poly (I:C) treatment increases the number of PBMCs that bind to the epithelial cell layer. This effect is much more evident in IPI-2I

cells than in IPEC-J2 cells, a result that is consistent with the larger production of HA in IPI-2I cells. To check whether PBMC adhesion is mediated by HA, the epithelial cell cultures were treated with hyaluronidase, an HA-degrading enzyme, before the binding assay. In this condition, PBMC binding was comparable to that of control cells, indicating that they bind to the HA produced by the epithelial cells.

The adhesion of PBMCs to IPI-21 cells was visualized by labelling of HA and CD44 followed by confocal microscopy (Figure 4). PBMCs were added to the Poly (I:C)-treated epithelial cells, incubated for 90 min, fixed and then labelled with HABP (green) and an antibody against CD44 (red). This receptor is expressed by PBMCs as well as by the epithelial cell surface. The presence of CD44 in the cell membrane of PBMCs is clearly visible. Figure 4A shows how PBMCs, clearly identified by the small size and round shape, bind to the areas where HA concentrates and even arrange along a HA cord-like structures (white arrows).

An image processing software was applied to confocal images to get more information about the three-dimensional relationship between these cell types. Figure 4B shows a closer vision of the adhered cells. PBMCs lay in the HA-coated epithelial cell surface in close contact with the HA network and, as shown in the zoomed images, PBMCs are partially surrounded or even embedded in the HA mesh.

To identify which cellular population within PBMCs is able to adhere to the Poly (I:C)-induced HA coat, we double-labelled HA and specific markers for the main cellular subsets in the PBMC population: CD20 (B cells), CD3 (T cells) and CD172a (monocytes/macrophages). As shown in Figure 5, the three subsets of cells are able to attach to the Poly (I:C)-induced HA matrix.

3.3. Effects of HA on cytokine production by PBMCs

PBMCs isolated from three different healthy pigs were treated with 0.1 or 0.4 mg/ml of either low or high molecular weight HA and the concentration of secreted cytokines in the conditioned media was measured by a competitive ELISA. LPS was used as

positive control. As shown in Figure 6, LMW-HA forms (100-150 kDa) clearly stimulate the secretion of TNF-α, IL-8 and IL-1β, which in basal conditions (control cells) is very low, whereas HMW-HA has no effect, at any of the two tested concentrations. IL-6 was below the detection limit of the technique. Interestingly, although the same trend is clearly observed for the three experiments, it is clear that there is individual variability in the response between the three pigs.

4. DISCUSSION

Over the last years, multiple reports have highlighted the role of HA as an active player on the modulation of inflammation. On one side, HA accumulates in inflamed tissues *in vivo,* and inflammatory stimuli induce *in vitro* the formation of a leukocyte-adhesive HA pericellular coat. At the same time, HA promotes epithelial protection and repair in the intestine and colon (Riehl et al., 2012). The intestine relies on HA not only to maintain homeostasis but also to generate innate responses, which are critical for defence when the intestinal barrier is damaged or attacked by pathogens (De La Motte and Kessler, 2015).

In this study, we hypothesized that this phenomenon takes place in porcine tissues and, therefore, it could also be involved in the mechanism of swine intestinal diseases. First of all, we have shown that porcine IECs or primary colonic mucosal SMCs treated with the viral mimetic Poly (I:C) generate a HA-based matrix associated to the cell membrane, as has been described for other cell types (de la Motte et al., 2003; De La Motte et al., 1999; Evanko et al., 2012, 2009; Lauer et al., 2009; Wang and Hascall, 2004). In basal conditions, colonic mucosal SMCs display the highest HA expression, whereas IECs have a lower expression of the polysaccharide, especially the IPEC-J2 cell line. The effect of Poly (I:C) treatment on pericellular HA induction was cell line-dependent and apparently related to the basal HA content of the cells. HA clearly coalesced into cable or fibril-like structures in SMC, as described in different

mesenchymal human cell types (De La Motte et al., 1999; Evanko et al., 2009). In epithelial cells, however, cables were not so evident and Poly (I:C)-induced HA appeared as a thicker pericellular coat. This effect was also different between the two IEC lines analyzed, as in non-differentiated IPEC-J2 cells, which hardly express HA in basal conditions, induction was very mild. The real three-dimensional structure of HA aggregates on the cell surfaces as a response to inflammatory stimuli is still under discussion, since the formation of cables could be, at least in part, due to lateral aggregation of HA chains during the fixation process (Evanko et al., 2009). Thus, it cannot be ruled out that the different appearance of the HA coat between IPI-2I cells and SMCs could rely on their different HA relative content, with a greater coalescence of HA into cables in SMCs due to their higher production.

We decided to work on IEC lines to study the effect of HA-induction on the adherence of PBMCs to the cell surface, since these cell lines are more homogeneous and easy to grow than primary mucosal SMCs. PBMCs adhere more avidly to IPI-2I cells than to IPEC-J2 cells, according to the higher effect of Poly (I:C) on HA induction in IPI-2I. Furthermore, hyaluronidase treatment confirmed that binding was specifically mediated by HA. The interaction between HA and PBMCs was visualized through labeling of PBMCs with an antibody against CD44 and confocal microscopy analysis. It is clearly observed that CD44-positive PBMCs are trapped by the newly induced HA coat. These results agree with those reported for human cells, where the interaction between Poly (I:C)-induced HA and monocytes has been shown to be predominantly mediated through the receptor CD44 (de la Motte et al., 2003; De La Motte et al., 1999). In our experimental model, monocytes, and T- and B-cells were found able to bind Poly (I:C)-induced HA matrices, as determined by staining bound PMBCs with specific markers for these cells (CD172a, CD3, and CD20 respectively). However, the individual binding affinity of each population could not be assessed, since an unknown percentage of adhered cells washed away as a result of the fixation step needed for the staining procedure.

IPEC-J2 cells cultured on permeable membranes undergo spontaneous differentiation, leading to the formation of polarised monolayers. This *in vitro* system is a good model to investigate the intestinal epithelial function, due to its similarities with the intestinal epithelial barrier *in vivo* (Vergauwen, 2015). On the contrary, the IPI-2I cell line is a transformed, non-polarised cell line (Boyen et al., 2009). We therefore tested the effect of Poly (I:C) on polarised IPEC-J2 cells, despite their low HA production in basal conditions and upon Poly (I:C) exposure when conventionally cultured. To this purpose cells were grown on collagen-coated PTFE permeable filters, which are the best *in vitro* system to compare with the *in vivo* situation (Geens and Niewold, 2011; Schierack et al., 2006). Interestingly, in this condition, IPEC-J2 cells responded to the viral mimic with a significant increase in HA production, which accumulated at the basolateral surface of cells, indicating that in a physiological situation, the recruitment of immune cells to the basolateral side of the epithelium may be mediated through binding to HA. Poly (I:C) also caused a disruption of the epithelial barrier, as demonstrated by the pronounced drop in TEER values. Decreased TEER values leading to increased gut permeability have been reported on rat ileal tissues *ex vivo* upon Poly (I:C) treatment (Moyano-Porcile et al., 2015).

The intestinal epithelium provides a first line of defence against external insults, and IECs play an important role in the inflammatory response after damage to the epithelial barrier, by activating defence mechanisms such as mucus production and production of cytokines and chemoattractants to recruit leukocytes to the site of infection (De La Motte and Kessler, 2015; Stadnyk, 2002). Preliminary results obtained in our laboratory indicate that IPI-2I and IPEC-J2 cells treated with Poly (I:C) show an increased production of IL-6 and IL-8, and that polarised IPEC-J2 cells after this treatment show changes compatibles with mucin overproduction (after Alcian-Blue/PAS staining) (unpublished results). Our results suggest that HA deposition after challenges constitute an attempt of the intestinal barrier to restore intestinal homeostasis and is involved in the innate response against pathogens also by contributing to the

recruitment of immune cells to the site of infection. This will be in accordance with the idea that HA-cables serve as a protective mechanism, controlling leukocyte activation by preventing their interaction with inflammation-promoting receptors (De La Motte et al., 1999; Day and de la Motte, 2005) and keeping them ready to be released in a controlled manner during the inflammatory reaction (Aya and Stern, 2014). Furthermore, this HA-based matrix may serve as a scaffold to prevent the loss of ECM components and scavengers of proinflammatory mediators (Day and de la Motte, 2005).

The adhesive HA coats can be induced by different stimuli, including viral infection, inflammation, endoplasmic reticulum stress or hyperglycemia (Majors et al., 2003; de la Motte et al., 2003; Wang & Hascall, 2004; Jokela et al., 2008; Lauer et al., 2009; Evanko et al., 2009). HA cable formation has been related to an increase in HA production through activation of HAS (Hascall et al., 2004; Stober et al., 2014), or to changes in HA accumulation without a net increase in HA production but depending on the interaction and cross-linking with its molecular partners (Day & de la Motte, 2005; Jokela et al., 2008; Evanko et al., 2009). Recently, Jokela et al. (2015) reported that the formation of an expanded and monocyte-adhesive HA coat in response to IL-1β in keratinocytes is controlled by cell-surface CD44. Thus, it is likely that different cellular responses are activated depending on the cell type and the nature of the stimulus, but the ultimately common effect is the recruitment of immune cells (Wang and Hascall, 2004).

In human medicine, the wide use of HA in medicine, surgery and cosmetics has driven research on the effects of HA on inflammation (Baeva et al., 2014). In general, published data support the conclusion that native HMW-HA is mostly protective and anti-inflammatory, whereas LMW-HA is pro-inflammatory and works as an alarm signal to the immune system. In this sense, we aimed to test the effect of low and high molecular-weight forms of HA (100-150 kDa and 2500 kDa respectively) on proinflammatory cytokine production by porcine PBMCs. Indeed, our results showed

438 that LMW-HA induces the production of TNF-α, IL-1β and IL-8 in contrast to HMW-HA.
439 Our results agree with the view that small fragments of HA with signalling properties
440 accumulate during inflammation, collaborating in the global output of the inflammatory
441 response. In this sense, the cross-linked HA structure present in the cables could be
442 more resistant to degradation than native HA, providing another limiting step in
443 inflammation (Day and de la Motte, 2005).
444 The contradictory effect of HA on inflammation may be understood with the different
445 functions of high and low molecular forms of HA (Turley et al., 2002; Toole, 2004; Jiang
446 et al., 2011). Low molecular weight HA fragments are thought to be involved in the
447 body's alarm system, transmitting various modes of "danger signals", related to
448 inflammatory and immunostimulatory functions (Stern et al., 2006). The repeating
449 disaccharide structure of HA has features of pathogen-associated molecular patterns
450 (PAMPs), which are recognized by TLR to initiate immune responses (Jiang et al.,
451 2011). This effect could be mediated through interaction with TLR4 (Termeer et al.,
452 2002; Taylor et al., 2004; Jiang et al., 2005) and CD44 (Yamawaki et al., 2009; Campo
453 et al., 2010). PBMCs express CD44 and TLR, including TLR2 and TLR4 (Uddin et al.,
454 2012; Yamawaki et al., 2009). In human PBMCs, stimulation with LMW-HA induced the
455 production of IL-6 and MCP-1 via both CD44 and TLR4, but through different
456 mechanisms (Yamawaki et al., 2009). To our knowledge, this is the first study where
457 the effect of HA on porcine immune cells is reported.
458 In conclusion, results presented here demonstrate that a) treatment of porcine
459 intestinal cells of epithelial and muscular mucosal origin respond to the viral mimic Poly
460 (I:C) by increasing HA deposition outside the cell, and that this effect is cell-dependent,
461 b) HA accumulates in the basolateral membrane of differentiated epithelial cells,
462 suggesting a physiological role *in vivo*, c) porcine PBMCs adhere to the HA-rich matrix
463 in a specific manner and d) HA can modulate the secretion of pro-inflammatory
464 cytokines by PBMCs in a size-specific manner. Altogether, these results indicate that

HA-dependent mechanisms may have a role in porcine intestinal protection and inflammatory and/or infectious diseases.

Aknowledgements

We are grateful to Dr. Félix García (Departament de Medicina i Cirurgia Animal, Facultat de Veterinària, UAB) for providing colon samples for the preparation of primary cell cultures and blood samples for PBMC isolation, Dr. Cristina Arce (Universidad de Córdoba, Spain) for providing the IPI-21 and IPEC-J2 cell lines, Dr. Maria Montoya (Centre de Recerca en Sanitat Animal, Barcelona, Spain) for providing Poly (I:C), Dr. Carol de la Motte (Lerner Research Institute, Cleveland, OH, USA) for providing the PBMC adhesion protocol and Dr. Alberto Marco and Dr. Francesc Accensi for providing the antibodies against CD20 and CD172a, respectively. We thank Dr. Enric Mateu for his helpful comments, and Dr. Mònica Roldán (Servei de Microscòpia (UAB)), the staff of the Histology laboratory (Facultat de Veterinària, UAB), and Ms. Anna Vilalta, Daniel Valent and Laura Arroyo for their assistance. This work was supported by grant AGL2011-30598-C03-02 from the Spanish Ministerio de Ciencia y Innovación and grant 2009SGR-1091 from the Generalitat de Catalunya. Part of the funding was financed by the FEDER program from the European Union.

Conflicts of interest: none.

493 **FIGURE LEGENDS**

494

495 **Figure 1. HA content and localization in IPEC-J2, IPI-2I and primary colon**
496 **mucosal SMCs (SMCs) treated with 20 µg/ml Poly (I:C).** Cells were treated with Poly
497 (I:C) for 18h and fixed. (A) HA was stained with DAB and cells were counterstained
498 with Mayer's haematoxylin, 400x magnification. (B) HA was labelled with Alexa Fluor®
499 488 (green) and cell nuclei were counterstained with Hoechst 33342 (blue). Images are
500 *z*-stack projections of serial *xy* sections. For IPEC-J2 images, optimized acquisition
501 conditions were used in order to minimize background (zoomed images), Scale bar =
502 20 μm). Images are representative of at least 5 independent experiments with similar
503 results. Arrows indicate the cable-like structures between SMC cells in close vicinity.

504

505 **Figure 2. Effects of Poly (I:C) on IPEC-J2 polarised cell monolayers cultured in**
506 **Transwell membranes.** (A) Effect of Poly (I:C) on monolayer integrity. TEER values
507 were measured in IPEC-J2 polarised monolayers treated or not with 20 µg/ml Poly (I:C)
508 for 18h. TEER values reflect a loss of epithelial integrity after exposure to Poly (I:C)
509 compared to control, untreated cells. Data are expressed as the mean ± SE of 9
510 replicates from 3 independent experiments. *** p <0.001. (B) Effect of Poly (I:C) on HA
511 deposition on IPEC-J2 polarised cells. HA was labelled with Alexa Fluor® 488 (green)
512 and cell nuclei were counterstained with Hoechst 33342 (blue). a, b) *z*-stack projections
513 of serial confocal *xy* sections of control and treated monolayers. Bar = 20 μm Poly
514 (I:C). c, d) Confocal images of control and treated monolayers processed with the
515 IMARIS software showing section views and three-dimensional volume
516 reconstructions.

517

518 **Figure 3. PBMC binding to Poly (I:C)-induced HA on porcine intestinal epithelial**
519 **cells.** Confluent IPI-2I and IPEC-J2 cell cultures were treated with Poly (I:C) for 18
520 hours at 37°C. Some wells were treated with hyaluronidase to confirm the specificity of

binging to HA. Porcine PBMCs were labelled with calcein and cell adhesion was quantified as described in Materials and Methods. Results from three independent experiments consisting in 4-6 replicates for each point are shown * $p \leq 0.05$, ** $p \leq 0.01$, *** $p \leq 0.001$.

Figure 4. PBMC binding to Poly (I:C)-induced HA on IPI-2I cells. IPI-2I cells were treated with DMEM/F12 medium containing 10% FBS with poly (I:C) for 18 hours at 37°C. PBMC cell adhesion was performed as described in Materials and Methods and observed by confocal microscopy. The IMARIS software was used for image processing. HA is labelled in green, CD44 in red and nuclei were stained with Hoechst (blue). (A) a) PBMCs appear as bright spheres attached to HA coat produced by the IPI-2I cells, which are attached to the culture plate. White arrows indicate groups of PBMCs arranged along a cord-like HA structure *z*-stack projection of serial *xy* confocal planes. b) Blend projection renders volume and a view of the surface of the cultures, where PBMCs lay embedded on top of the HA coat that surround the intestinal cells. (B) a) Closer view of HA-mediated attachment of PBMCs to poly (I:C)-treated IPI-2I cells. *z*-stack projection of serial *xy* confocal planes. b) The section view show *xz* and *yz* lateral planes with PBMCs attached to the HA-coated monolayer. c) Blend projection showing a view of the culture surface. d) Three-dimensional reconstruction showing the interaction between the HA mesh and PBMCs. Zoomed and rotated image shows an isolated PBMC embedded in the HA coat.

Figure 5. Identification of PBMC subpopulations adhered to the Poly (I:C)-induced HA coat. PBMCs were added to Poly (I:C)-IPI-2I-treated cells and left to adhere, fixed and double stained for HA (green) and markers against 3 different PBMCs subtypes (red): CD3 for T-cells, CD20 for B-cells and CD172a for monocytic cells. Images are *z*-stack projections of serial *xy* sections Two images for each marker are shown. Bar = 10 μm.

549

550 **Figure 6. Cytokine production by porcine PBMCs treated with low- and high**
551 **molecular weight forms of HA.** Porcine PBMCs were plated and incubated with low-
552 molecular weight HA (100-150 kDa) or high molecular weight HA (2500 kDa) or LPS as
553 described in Materials and Methods for 24 h at 37°C. The concentration of cytokines
554 was determined in culture supernatants by specific ELISA assays. The experiment was
555 performed three times and a scatter plot of all results is shown, with each experiment
556 marked with one colour. *$p \leq 0.05$, ** $p \leq 0.01$, ***$p \leq 0.001$
557

References

Aruffo, A., Stamenkovic, I., Melnick, M., Underhill, C.B., Seed, B., 1990. CD44 is the principal cell surface receptor for hyaluronate. Cell 61, 1303–1313.

Aya, K.L., Stern, R., 2014. Hyaluronan in wound healing: Rediscovering a major player. Wound Repair Regen. 1–54. doi:10.1111/wrr.12214

Baeva, L.F., Lyle, D.B., Rios, M., Langone, J.J., Lightfoote, M.M., 2014. Different molecular weight hyaluronic acid effects on human macrophage interleukin 1β production. J. Biomed. Mater. Res. - Part A 102, 305–314.

Boyen, F., Pasmans, F., Van Immerseel, F., Donné, E., Morgan, E., Ducatelle, R., Haesebrouck, F., 2009. Porcine in vitro and in vivo models to assess the virulence of Salmonella enterica serovar Typhimurium for pigs. Lab. Anim. 43, 46–52.

Campo, G.M., Avenoso, A., Campo, S., D'Ascola, A., Nastasi, G., Calatroni, A., 2010. Small hyaluronan oligosaccharides induce inflammation by engaging both toll-like-4 and CD44receptors in human chondrocytes. Biochem Pharmacol. 80, 480-90.

Day, A.J., de la Motte, C.A., 2005. Hyaluronan cross-linking: a protective mechanism in inflammation? Trends Immunol. 26, 637–643.

De La Motte, C.A., Hascall, V.C., Calabro, A., Yen-Lieberman, B., Strong, S.A., 1999. Mononuclear leukocytes preferentially bind via CD44 to hyaluronan on human intestinal mucosal smooth muscle cells after virus infection or treatment with poly(I:C). J. Biol. Chem. 274, 30747–30755.

De la Motte, C.A., Hascall, V.C., Drazba, J., Bandyopadhyay, S.K., Strong, S.A., 2003. Mononuclear leukocytes bind to specific hyaluronan structures on colon mucosal smooth muscle cells treated with polyinosinic acid:polycytidylic acid: inter-alpha-trypsin inhibitor is crucial to structure and function. Am. J. Pathol. 163, 121–133.

De La Motte, C.A., Kessler, S.P., 2015. The role of hyaluronan in innate defense responses of the intestine. Int. J. Cell Biol. doi: 10.1155/2015/481301

Erickson, M., Stern, R., 2012. Chain gangs: New aspects of hyaluronan metabolism. Biochem. Res. Int. doi:10.1155/2012/893947

Evanko, S.P., Potter-Perigo, S., Bollyky, P.L., Nepom, G.T., Wight, T.N., 2012. Hyaluronan and versican in the control of human T-lymphocyte adhesion and migration. Matrix Biol. 31, 90–100.

Evanko, S.P., Potter-Perigo, S., Johnson, P.Y., Wight, T.N., 2009. Organization of hyaluronan and versican in the extracellular matrix of human fibroblasts treated with the viral mimetic poly I:C. J. Histochem. Cytochem. 57, 1041–1060.

Geens, M.M., Niewold, T.A., 2011. Optimizing culture conditions of a porcine epithelial cell line IPEC-J2 through a histological and physiological characterization. Cytotechnology 63, 415–423.

595 Hascall, V.C., Majors, A.K., De La Motte, C.A., Evanko, S.P., Wang, A., Drazba, J.A.,
596 Strong, S.A., Wight, T.N., 2004. Intracellular hyaluronan: a new frontier for
597 inflammation? Biochim. Biophys. Acta 1673, 3–12.

598 Jiang, D., Liang, J., Fan, J., Yu, S., Chen, S., Luo, Y., Prestwich, G.D., Mascarenhas,
599 M.M., Garg, H.G., Quinn, D.A., Homer, R.J., Goldstein, D.R., Bucala, R., Lee,
600 P.J., Medzhitov, R., Noble, P.W., 2005. Regulation of lung injury and repair by
601 Toll-like receptors and hyaluronan. Nat. Med. 11, 1173–1179.

602 Jiang, D., Liang, J., Noble, P.W., 2011. Hyaluronan as an immune regulator in human
603 diseases. Physiol. Rev. 91, 221–264.

604 Jiang, D., Liang, J., Noble, P.W., 2007. Hyaluronan in tissue injury and repair. Annu.
605 Rev. Cell Dev. Biol. 23, 435–461.

606 Jokela, T.A., Lindgren, A., Rilla, K., Maytin, E., Hascall, V.C., Tammi, R.H., Tammi,
607 M.I., 2008. Induction of hyaluronan cables and monocyte adherence in epidermal
608 keratinocytes. Connect. Tissue Res. 49, 115–119.

609 Jokela, T., Oikari, S., Takabe, P., Rilla, K., Kärnä, R., Tammi, M., Tammi, R., 2015.
610 Interleukin-1β-induced Reduction of CD44 Ser-325 Phosphorylation in Human
611 Epidermal Keratinocytes Promotes CD44 Homomeric Complexes, Binding to
612 Ezrin, and Extended, Monocyte-adhesive Hyaluronan Coats. J. Biol. Chem. 290:
613 12379–93.

614 Kaeffer, B., Bottreau, E., Velge, P., Pardon, P., 1993. Epithelioid and fibroblastic cell
615 lines derived from the ileum of an adult histocompatible miniature boar (d/d
616 haplotype) and immortalized by SV40 plasmid. Eur. J. Cell Biol. 62, 152–162.

617 Kessler, S., Rho, H., West, G., Fiocchi, C., Drazba, J., de la Motte, C., 2008.
618 Hyaluronan (HA) deposition precedes and promotes leukocyte recruitment in
619 intestinal inflammation. Clin. Transl. Sci. 1, 57–61.

620 Lauer, M.E., Mukhopadhyay, D., Fulop, C., de la Motte, C.A., Majors, A.K., Hascall,
621 V.C., 2009. Primary murine airway smooth muscle cells exposed to poly(I,C) or
622 tunicamycin synthesize a leukocyte-adhesive hyaluronan matrix. J. Biol. Chem.
623 284, 5299–5312.

624 Majors, A.K., Austin, R.C., de la Motte, C.A., Pyeritz, R.E., Hascall, V.C., Kessler, S.P.,
625 Sen, G., Strong, S.A., 2003. Endoplasmic reticulum stress induces hyaluronan
626 deposition and leukocyte adhesion. J. Biol. Chem. 278, 47223–47231.

627 Mohamadzadeh, M., DeGrendele, H., Arizpe, H., Estess, P., Siegelman, M., 1998.
628 Proinflammatory stimuli regulate endothelial hyaluronan expression and
629 CD44/HA-dependent primary adhesion. J. Clin. Invest. 101, 97–108.

630 Moyano-Porcile, V., Olavarria-Ramirez, L., Gonzalez-Arancibia, C., Bravo, J.A., Julio-
631 Pieper, M., 2015. Short-term effects of Poly(I:C) on gut permeability. Pharmacol.
632 Res. 101, 130–136.

633 Petrey, A.C., de la Motte, C.A., 2014. Hyaluronan, a crucial regulator of inflammation.
634 Front. Immunol. 5, 101.

635 Potter-Perigo, S., Johnson, P.Y., Evanko, S.P., Chan, C.K., Braun, K.R., Wilkinson,
636 T.S., Altman, L.C., Wight, T.N., 2010. Polyinosine-polycytidylic acid stimulates
637 versican accumulation in the extracellular matrix promoting monocyte adhesion.
638 Am. J. Respir. Cell Mol. Biol. 43, 109–120.

639 Rhoads, J.M., Chen, W., Chu, P., Berschneider, H.M., Argenzio, R.A., Paradiso, A.M.,
640 1994. L-glutamine and L-asparagine stimulate Na+ -H+ exchange in porcine
641 jejunal enterocytes. Am. J. Physiol. 266, G828–38.

642 Riehl, T.E., Ee, X., Stenson, W.F., 2012. Hyaluronic acid regulates normal intestinal
643 and colonic growth in mice. AJP Gastrointest. Liver Physiol. 303: G377–G388.

644 Schierack, P., Nordhoff, M., Pollmann, M., Weyrauch, K.D., Amasheh, S., Lodemann,
645 U., Jores, J., Tachu, B., Kleta, S., Blikslager, A., Tedin, K., Wieler, L.H., 2006.
646 Characterization of a porcine intestinal epithelial cell line for in vitro studies of
647 microbial pathogenesis in swine. Histochem. Cell Biol. 125, 293–305.

648 Stadnyk, A.W., 2002. Intestinal epithelial cells as a source of inflammatory cytokines
649 and chemokines. Can J Gastroenterol 16, 241–246.

650 Stern, R., Asari, A.A., Sugahara, K.N., 2006. Hyaluronan fragments: an information-rich
651 system. Eur. J. Cell Biol. 85, 699–715.

652 Stern, R., Kogan, G., Jedrzejas, M.J., Šoltés, L., 2007. The many ways to cleave
653 hyaluronan. Biotechnol. Adv. 25, 5375–57.

654 Stober, V.P., Szczesniak, C., Childress, Q., Heise, R.L., Bortner, C.D., Hollingsworth,
655 J.W., Neuringer, I.P., Palmer, S.M., Garantziotis, S., 2014. Bronchial Epithelial
656 Injury in the Context of Alloimmunity Promotes Lymphocytic Bronchiolitis through
657 Hyaluronan Expression. Am. J. Physiol. Lung Cell. Mol. Physiol.
658 doi:10.1152/ajplung.00353.2013

659 Taylor, K.R., Trowbridge, J.M., Rudisill, J.A., Termeer, C.C., Simon, J.C., Gallo, R.L.,
660 2004. Hyaluronan Fragments Stimulate Endothelial Recognition of Injury through
661 TLR4. J. Biol. Chem. 279, 17079–17084.

662 Termeer, C., Benedix, F., Sleeman, J., Fieber, C., Voith, U., Ahrens, T., Miyake, K.,
663 Freudenberg, M., Galanos, C., Simon, J.C., 2002. Oligosaccharides of Hyaluronan
664 activate dendritic cells via toll-like receptor 4. J. Exp. Med. 195, 99–111.

665 Toole, B.P., 2004. Hyaluronan: from extracellular glue to pericellular cue. Nat. Rev. 4,
666 528–539.

667 Turley, E.A., Noble, P.W., Bourguignon, L.Y., 2002. Signaling properties of hyaluronan
668 receptors. J. Biol. Chem. 277, 4589–4592.

669 Uddin, M.J., Nuro-Gyina, P.K., Islam, M.A., Tesfaye, D., Tholen, E., Looft, C.,
670 Schellander, K., Cinar, M.U., 2012. Expression dynamics of Toll-like receptors
671 mRNA and cytokines in porcine peripheral blood mononuclear cells stimulated by
672 bacterial lipopolysaccharide. Vet. Immunol. Immunopathol. 147, 211–222.

673 Vergauwen, H., 2015. The IPEC-J2 cell line, in: The Impact of Food Bioactives on
674 Health: In Vitro and Ex Vivo Models. doi:10.1007/978-3-319-16104-4_12

675

676 Wang, A., Hascall, V.C., 2004. Hyaluronan Structures Synthesized by Rat Mesangial
677 Cells in Response to Hyperglycemia Induce Monocyte Adhesion. J. Biol. Chem.
678 279, 10279–10285.

679 Yamawaki, H., Hirohata, S., Miyoshi, T., Takahashi, K., Ogawa, H., Shinohata, R.,
680 Demircan, K., Kusachi, S., Yamamoto, K., Ninomiya, Y., 2009. Hyaluronan
681 receptors involved in cytokine induction in monocytes. Glycobiology 19, 83–92.

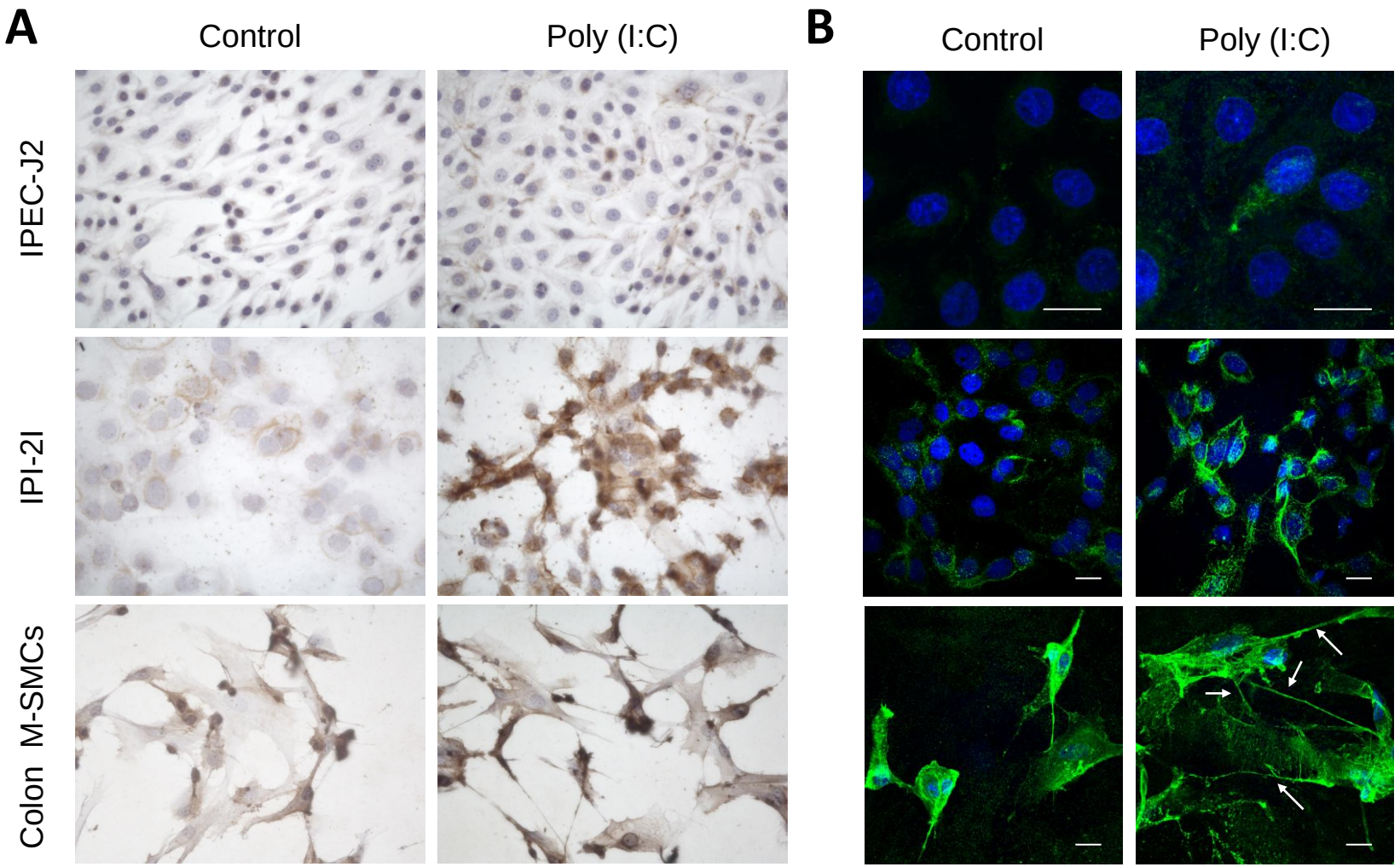


Figure 1

Figure 2A

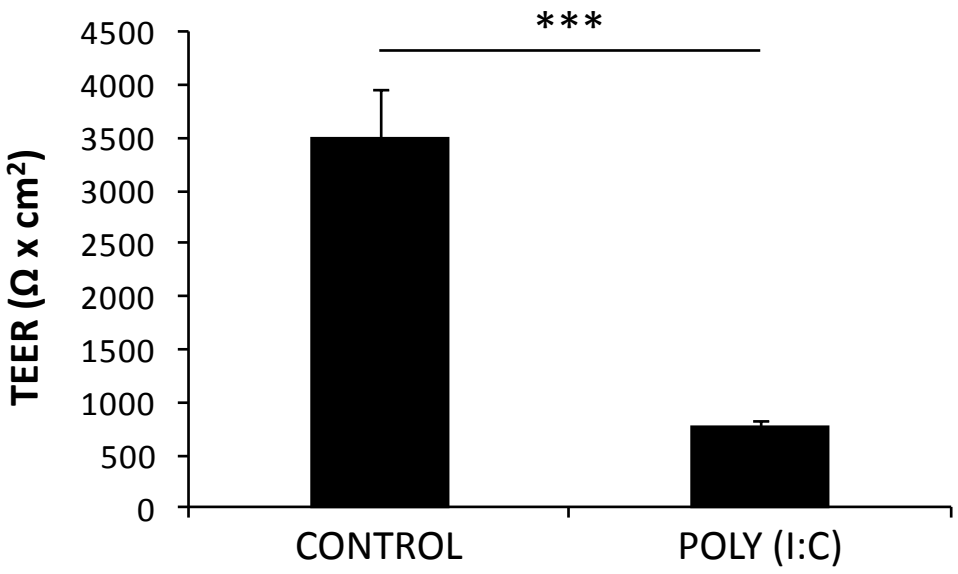


Figure 2A

Figure 2B

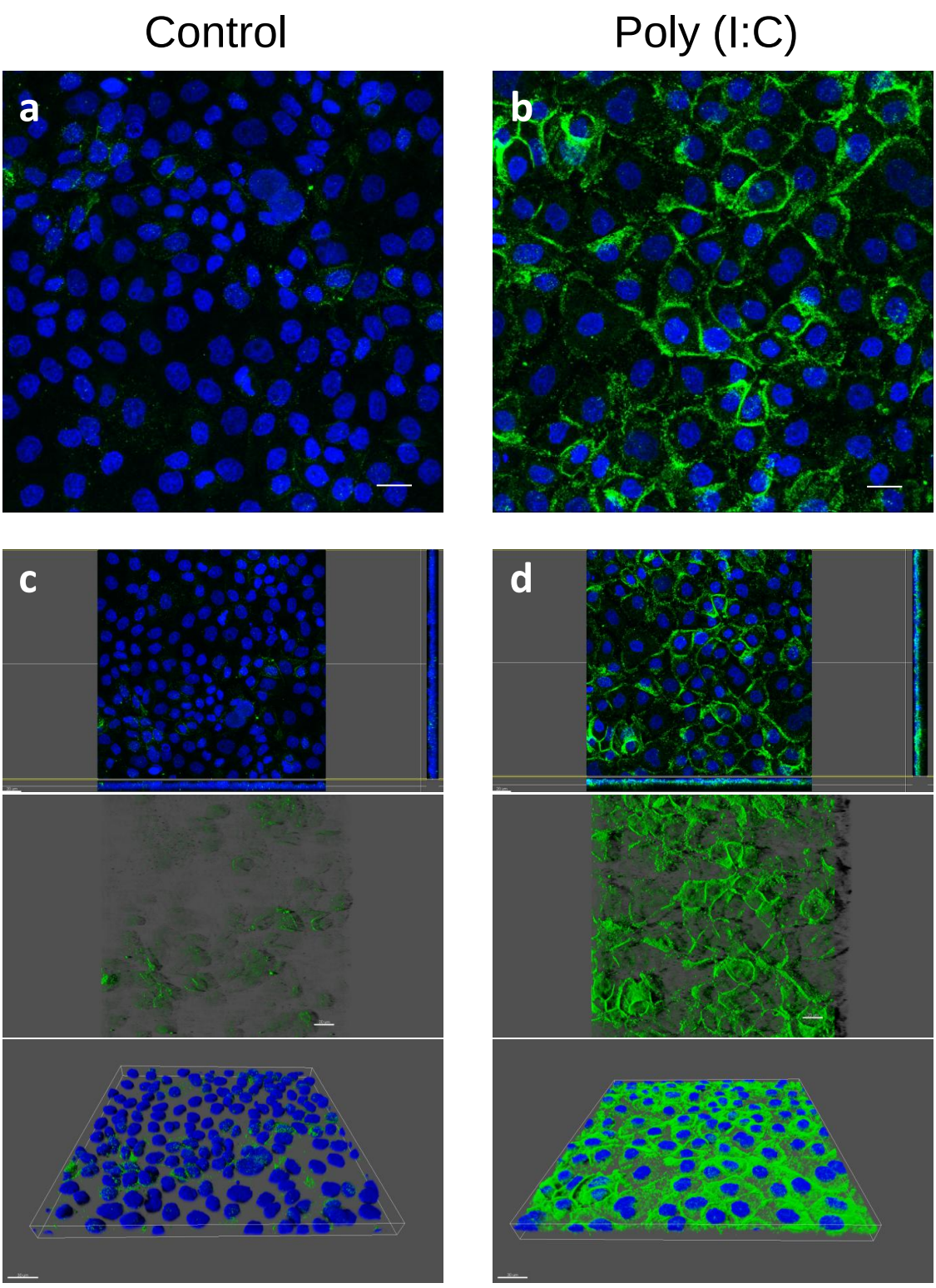


Figure 2B

Figure 3

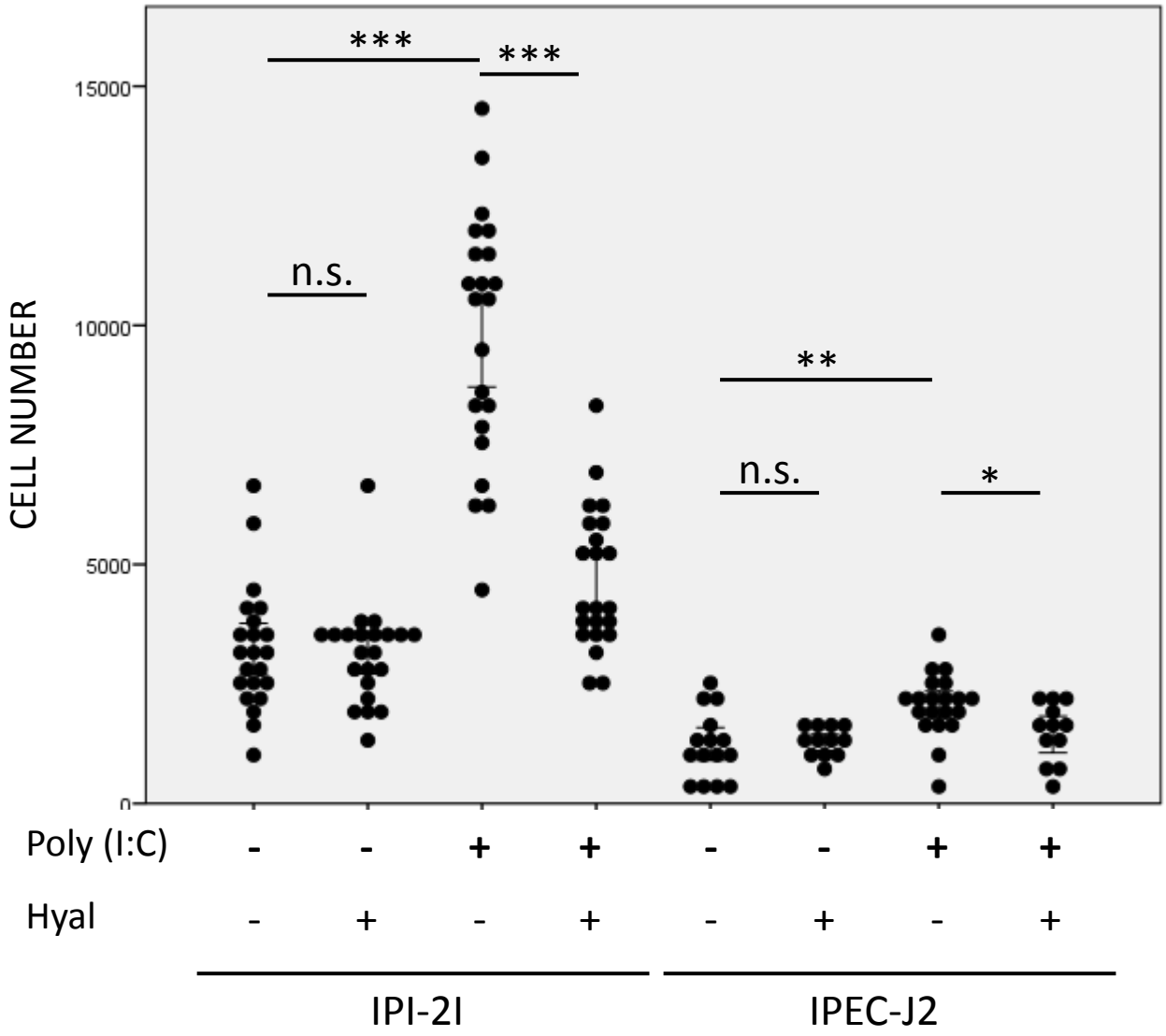


Figure 3

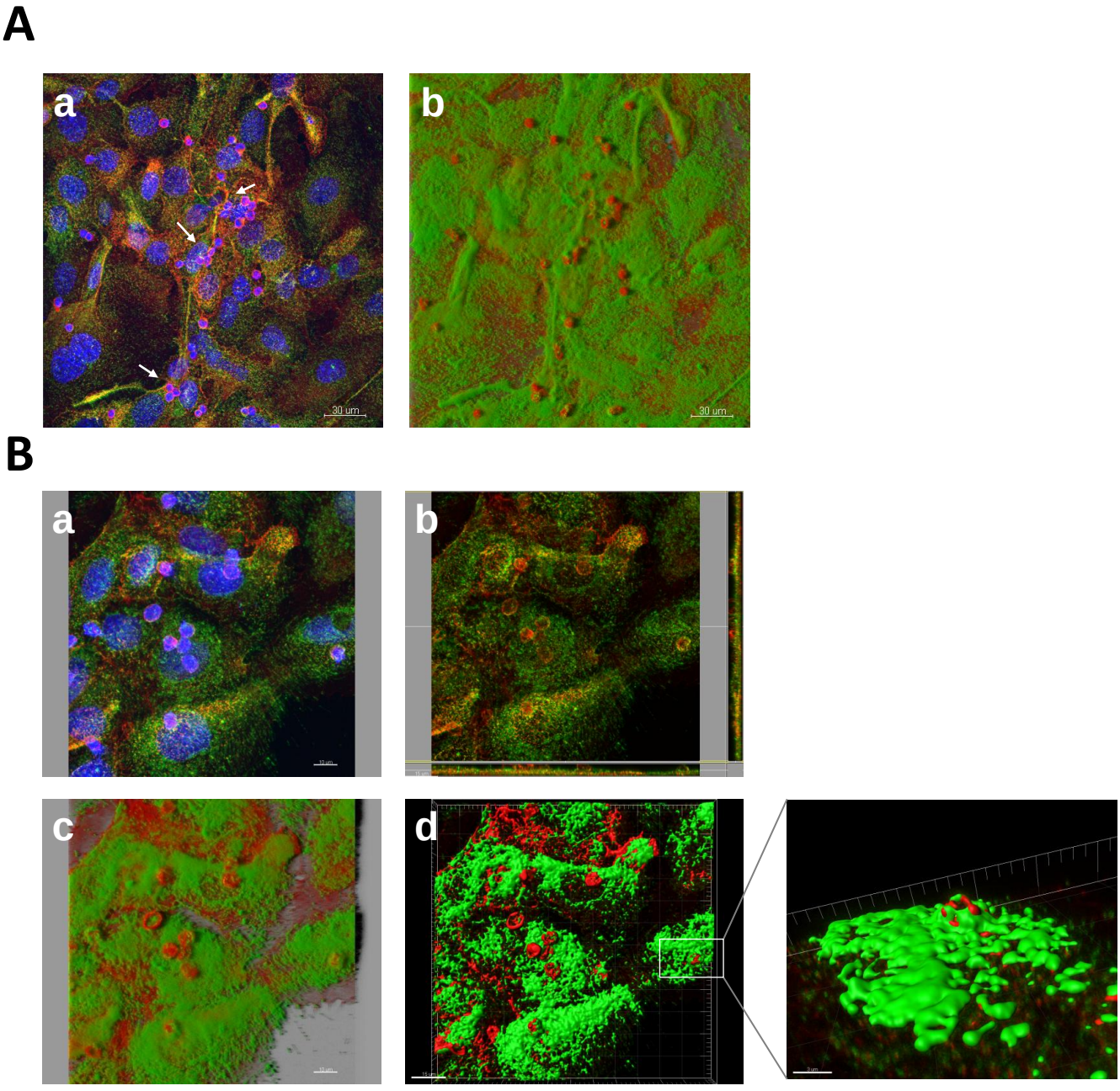


Figure 4

Figure 5

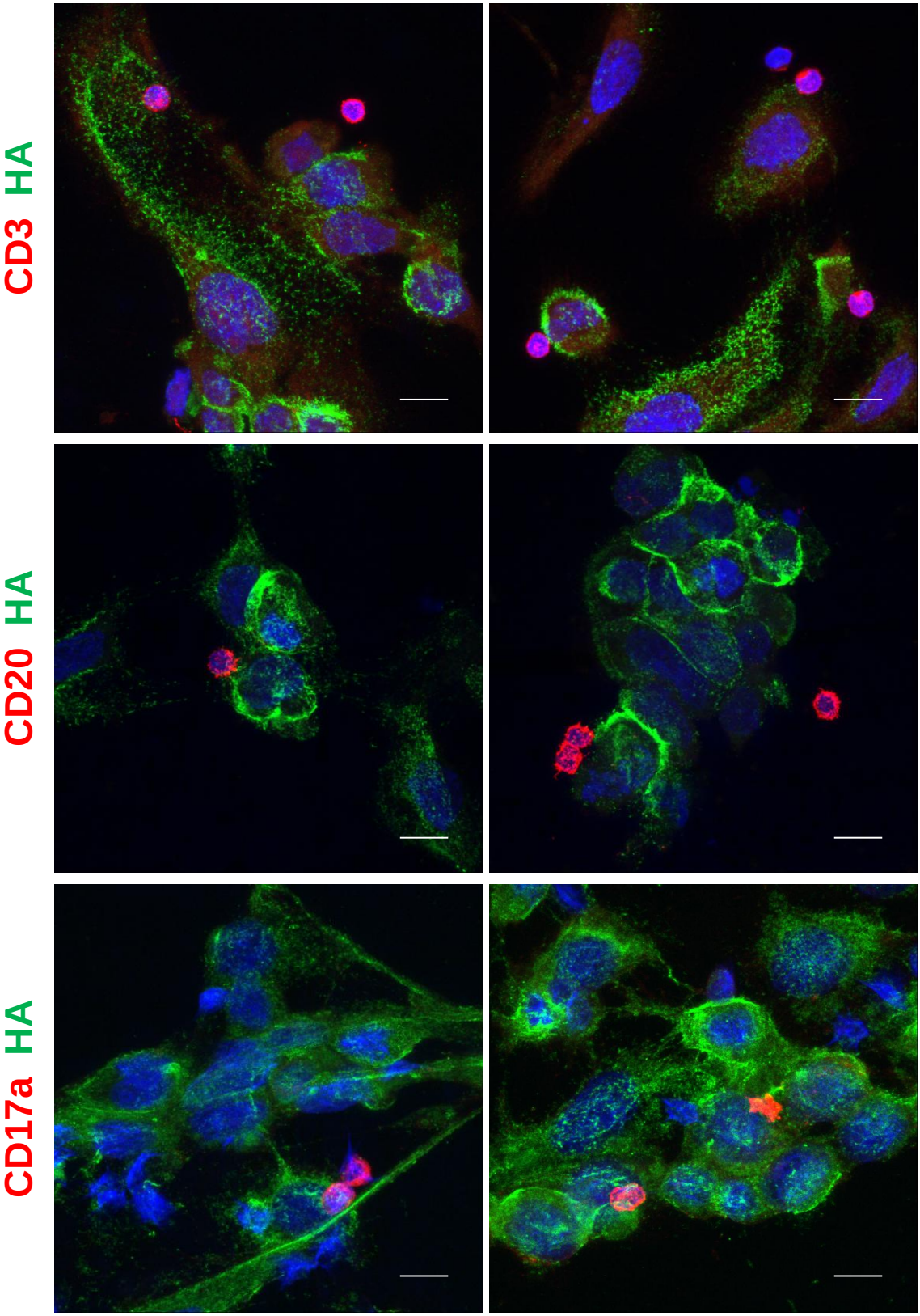
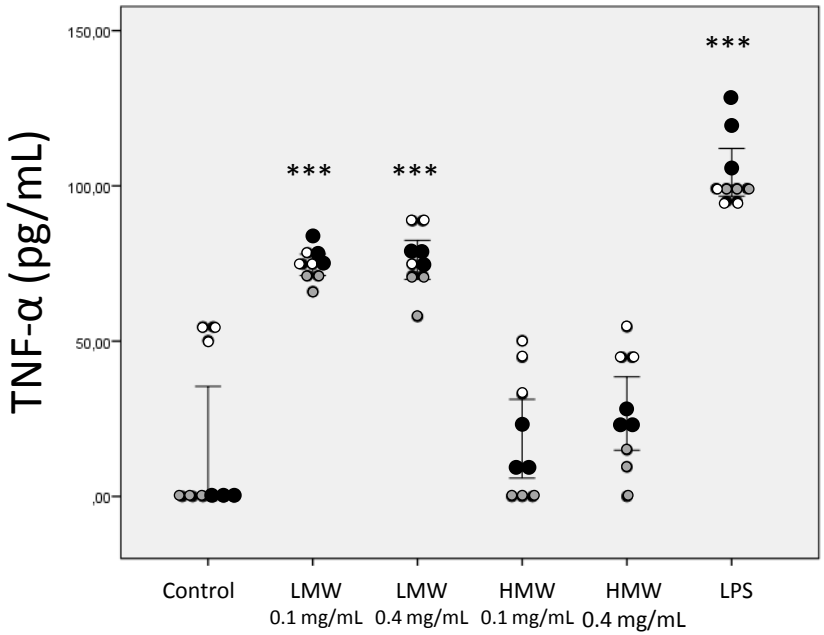
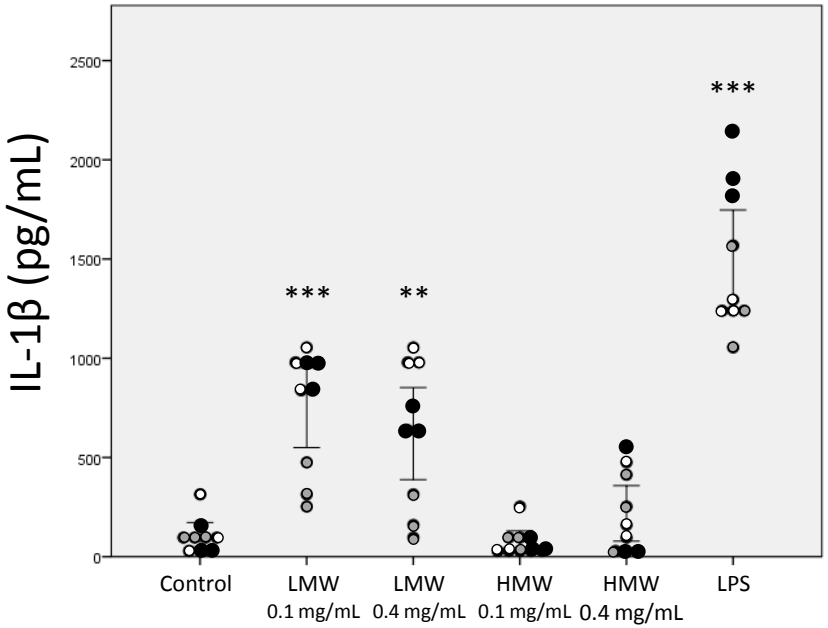


Figure 5

Figure 6





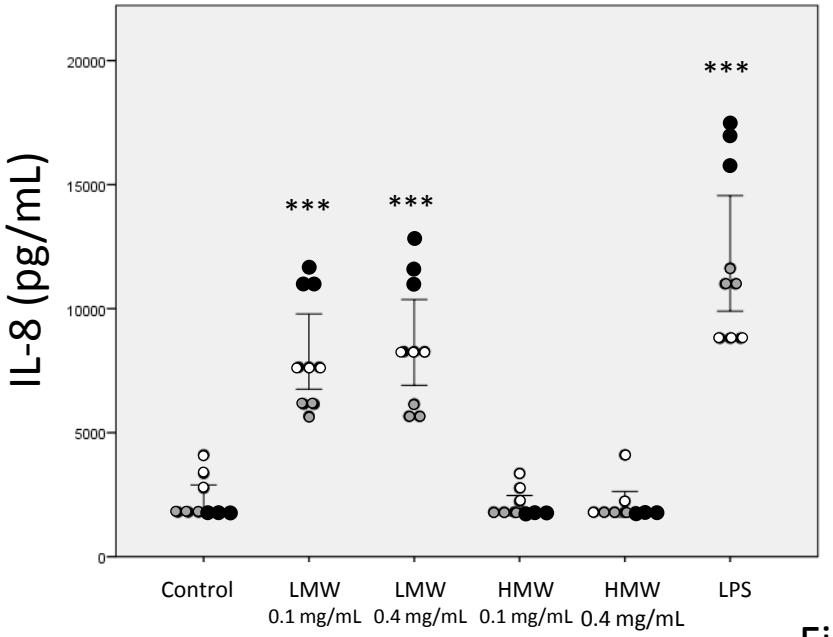


Figure 6

Highlights

- Poly (I:C) induces the deposition of hyaluronan in the surface of porcine intestinal cells
- Poly (I:C)-induced hyaluronan coats in intestinal cells are adhesive for porcine PBMCs
- Low molecular weight hyaluronan fragments promote the secretion of proinflammatory cytokines in porcine PBMCs.

Graphical Abstract

